Full Paper

Applied Organometallic Chemistry

Received: 13 December 2014 Revised: 26 December 2014 Accepted: 29 December 2014 Published online in Wiley Online Library

(wileyonlinelibrary.com) DOI 10.1002/aoc.3282

A highly stable and efficient magnetically recoverable and reusable Pd nanocatalyst in aqueous media heterogeneously catalysed Suzuki C–C cross-coupling reactions

Bahareh Abbas Khakiani[a], Khalil Pourshamsian[a] and Hojat Veisi[b]*

Surface modification of Fe_3O_4 nanoparticles with triethoxyethylcyanide groups was used for the immobilization of palladium nanoparticles to produce Fe_3O_4/Ethyl-CN/Pd. The catalyst was characterized using Fourier transform infrared, wavelength-dispersive X-ray, energy-dispersive X-ray and X-ray photoelectron spectroscopies, field-emission scanning electron and transmission electron microscopies, and X-ray diffraction, vibrating sample magnetometry and inductively coupled plasma analyses. In this fabrication, cyano groups played an important role as a capping agent. The catalytic behaviour of Fe_3O_4/Ethyl-CN/Pd nanoparticles was measured in the Suzuki cross-coupling reaction of various aryl halides (Ar–I, Ar–Br, Ar–Cl) with phenylboronic acid in aqueous phase at room temperature. Interestingly, the novel catalyst could be recovered in a facile manner from the reaction mixture by applying an external magnet device and recycled seven times without any significant loss in activity.

Keywords: immobilized palladium catalyst; magnetic nanoparticles; heterogeneous catalyst; recyclable; Suzuki reaction

Introduction

The Suzuki reaction is one of the most versatile and utilized reactions for the selective construction of carbon–carbon bonds,[1–4] in particular for the construction of biaryls,[4–7] since these have a diverse spectrum of applications,[8] ranging from pharmaceuticals to materials science. Therefore, the development of easily available or prepared, inexpensive catalysts, and environmentally benign solvents and methodology avoiding the use of expensive and toxic ligands remain a highly desirable goal. Recently, various catalytic systems have been reported for Suzuki coupling reactions.[9,10]

Development of this reaction is greatly dependent on the reactivity of the palladium catalyst. Generally, catalysts are divided into two groups: most examples are homogeneous systems and the others are heterogeneous systems. Despite the observed beneficial effects with homogeneous catalysts, problems associated with the separation and recovery of the expensive active catalyst limit their use in industrial and synthetic applications. In light of this, continuing efforts are now being made to carry out the reactions with heterogeneous systems to aid recovery, recyclability and re-use of the catalyst. Immobilization of homogeneous catalysts on various insoluble supports (especially porous materials with high surface areas) can lead to simple catalyst recycling via filtration or centrifugation. However, a substantial decrease in the activity of the immobilized catalyst is frequently observed due to the loss of the catalyst in the separation processes and/or to diffusion factors. In an attempt to resolve such problems, nanoparticles have been used as alternative soluble matrixes for supporting homogeneous catalysts. When the size of the support materials is decreased to the nanometre scale, the surface area of nanoparticles will increase dramatically. As a consequence, nanoparticles can have higher catalyst loading capacity and higher dispersion than many conventional support matrixes, leading to the improved catalytic activity of the supported catalysts. However, conventional separation methods may become inefficient for support particle sizes below 100 nm. The incorporation of magnetic nanoparticles (MNPs) into supports offers a solution to this problem. The renewed interest in synthesis of MNPs is due to their technological applications such as data storage, biological imaging and biomedicine.[11–15] One of the attractive features of MNPs is the possibility of fast and cost-efficient separation by applying an external magnetic field, which makes them ideal candidates for practical use in catalysis processes. This new direction in catalysis has galvanized academic research and led to the development of a great number of magnetic-based catalysts, especially magnetite (Fe_3O_4) that has found application in various reactions.[16–25] Several accounts of the synthesis, characterization and application of Fe_3O_4 MNPs utilized in coupling reactions have been reported in the literature.[26–37]

It should be noted that magnetostatic interactions between particles make Fe_3O_4 particles susceptible to agglomeration. On the other hand, the oxidation of Fe^{2+} causes depletion of the magnetism of Fe_3O_4. Thus, in order to decrease the degree of

* Correspondence to: Hojat Veisi, Department of Chemistry, Payame Noor University, Tehran, Iran. E-mail: hojatveisi@yahoo.com

a Department of Chemistry, Tonekabon Branch, Islamic Azad University, Tonekabon, Iran

b Department of Chemistry, Payame Noor University, Tehran, Iran

agglomeration and increase the oxidation resistance, effective coating of magnetite particles is essential.

In this context, we considered that Fe_3O_4 supporting ethyl cyanide groups (Fe_3O_4/Ethyl-CN) would serve as an efficient and robust support material for metal ions. Our interest in this area[38–43] has prompted us to explore the immobilization of $PdCl_2$ on the surface of Fe_3O_4/Ethyl-CN. Here, we report a convenient procedure for synthesizing a recoverable Fe_3O_4/Ethyl-CN/Pd nanocatalyst for the Suzuki coupling reaction in a green medium (H_2O–EtOH). More importantly, the synthesized Fe_3O_4/Ethyl-CN/Pd nanocomposite has good magnetic property, and can be easily separated from the reaction mixture using a magnet. By utilizing this property, it can be reused for seven cycles without loss of catalytic activity, indicative of potential application in industry.

Experimental

Preparation of Fe_3O_4 MNPs

Naked Fe_3O_4 nanoparticles were prepared by chemical co-precipitation of Fe^{3+} and Fe^{2+} ions with a molar ratio of 2:1. Typically, $FeCl_3{\cdot}6H_2O$ (5.838 g, 0.0216 mol) and $FeCl_2{\cdot}4H_2O$ (2.147 g, 0.0108 mol) were dissolved in 100 ml of deionized water at 85°C under nitrogen atmosphere and with vigorous mechanical stirring (500 rpm). Then, 10 ml of 25% NH_4OH was quickly injected into the reaction mixture in one portion. The addition of the base to the Fe^{2+}/Fe^{3+} salt solution resulted in the immediate formation of a black precipitate of MNPs. The reaction continued for another 25 min and the mixture was cooled to room temperature. Subsequently, the resultant ultrafine magnetic particles were treated by magnetic separation and washed several times with deionized water.

Preparation of Fe_3O_4/Ethyl-CN

The obtained MNP powder (500 mg) was dispersed in 50 ml of toluene solution by sonication for 20 min, and then triethoxyethylcyanide (3 mmol) was added to the mixture. The mixture was refluxed under argon atmosphere at 100°C for 48 h. The product was separated by filtration, washed with ethanol and dried under vacuum for 24 h at 50°C. The precipitated product (Fe_3O_4/Ethyl-CN) was dried at room temperature under vacuum.

Preparation of Fe_3O_4/Ethyl-CN/Pd(0)

Fe_3O_4/Ethyl-CN (500 mg) was dispersed in CH_3CN (30 ml) in an ultrasonic bath for 30 min. Subsequently, a yellow solution of $PdCl_2$ (30 mg) in 30 ml of CH_3CN was added to the dispersion of Fe_3O_4/Ethyl-CN and the mixture was stirred for 10 h at 20–25°C. Then, the Fe_3O_4/Ethyl-CN/Pd(II) thus obtained was separated using magnetic decantation and washed with CH_3CN, water and acetone successively to remove the unattached substrates.

The reduction of Fe_3O_4/Ethyl-CN/Pd(II) using hydrazine hydrate was performed as follows. Fe_3O_4/Ethyl-CN/Pd(II) (50 mg) was dispersed in 60 ml of water, and then 100 μl of hydrazine hydrate (80%) was added. The pH of the mixture was adjusted to 10 with 25% ammonium hydroxide and the reaction was carried out at 95°C for 2 h. The final product, Fe_3O_4/Ethyl-CN/Pd(0), was washed with water and dried in vacuum at 40°C. Scheme 1 depicts the synthetic procedure for Fe_3O_4/Ethyl-CN/Pd. The concentration of palladium in Fe_3O_4/Ethyl-CN/Pd was 2.75 wt% (0.27 mmol g^{-1}), which was determined using inductively coupled plasma atomic emission spectroscopy (ICP-AES) and energy dispersive X-ray spectroscopy (EDS).

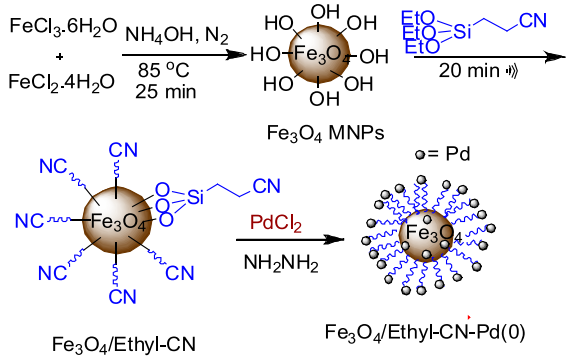

Scheme 1. Preparation of Fe_3O_4/Ethyl-CN/Pd nanocatalyst.

Suzuki–Miyaura Coupling Reaction

In a typical reaction, 7 mg of Fe_3O_4/Ethyl-CN/Pd (0.0021 mmol Pd) was placed in a 25 ml Schlenk tube, to which was added 1 mmol of aryl halide in 5 ml of water–ethanol (1:1), 0.134 g (1.1 mmol) of phenylboronic acid and 0.276 mg (2 mmol) of K_2CO_3. The mixture was then stirred for the desired time at 20–25°C. The reaction was monitored using TLC. After completion of the reaction, 5 ml of ethanol was added, and the catalyst was removed using an external magnet. Further purification was achieved with column chromatography.

Results and Discussion

Fe_3O_4/Ethyl-CN/Pd was prepared using the concise route outlined in Scheme 1. Naked Fe_3O_4 MNPs were prepared through a chemical co-precipitation method, and subsequently coated with 2-cyanoethyltriethoxysilane to achieve cyanoethyl-functionalized MNPs. Ultimately, the reaction of cyano groups with $PdCl_2$ and subsequent its reduction led to the corresponding Pd nanoparticles supported on MNPs. Finally, the mixture was collected using an external magnet, followed by drying in vacuum. The Pd content in Fe_3O_4/Ethyl-CN/Pd catalyst was determined as 2.75 wt% (0.27 mmol

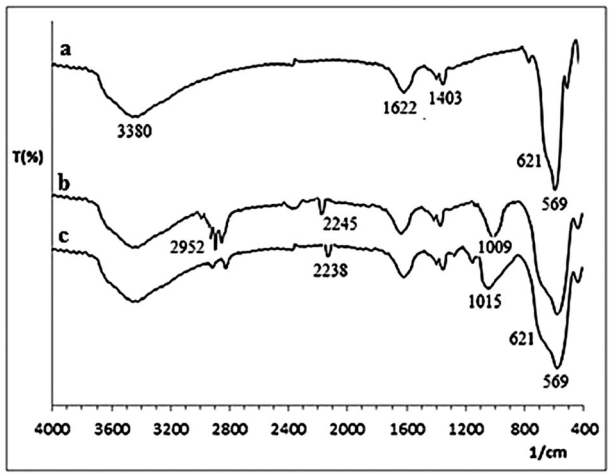

Figure 1. FT-IR spectra of (a) Fe_3O_4, (b) Fe_3O_4/Ethyl-CN and (c) Fe_3O_4/Ethyl-CN/Pd.

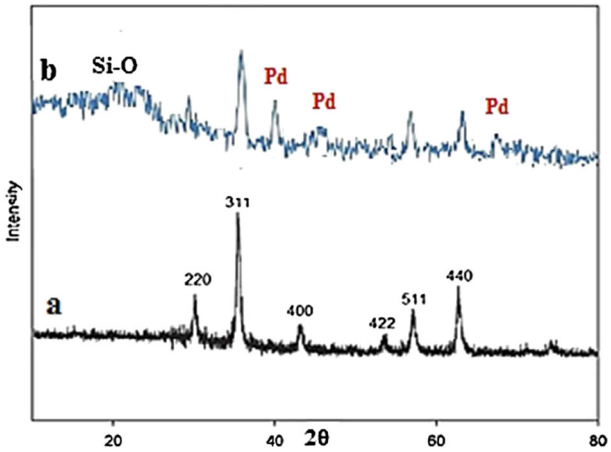

Figure 2. XRD patterns of (a) Fe_3O_4 and (b) Fe_3O_4/Ethyl-CN/Pd.

g^{-1}) using ICP-AES. The characterization of the catalyst was carried out using Fourier transform infrared (FT-IR) spectroscopy, wavelength-dispersive X-ray spectroscopy (WDX), EDS, X-ray photoelectron spectroscopy (XPS), X-ray diffraction (XRD), field-emission scanning electron microscopy (FESEM), transmission electron microscopy (TEM), ICP and vibrating sample magnetometry (VSM).

Figure 1 shows the FT-IR spectra for MNPs, MNPs/Ethyl-CN and MNPs/Ethyl-CN/Pd. The FT-IR spectrum for the MNPs alone shows a stretching vibration at 3381 cm^{-1} which incorporates contributions from both symmetric and asymmetric modes of the O–H bonds which are attached to the surface iron atoms.[44] The bands at low wavenumbers ($\leq$700 cm^{-1}) come from vibrations of Fe–O bonds of iron oxide, which for bulk Fe_3O_4 samples appear at 570 and 375 cm^{-1}, but for Fe_3O_4 nanoparticles are blue-shifted to 624 and 572 cm^{-1} due to the size reduction.[45–47] The presence of an adsorbed water layer is confirmed by a stretching vibrational mode of water at 1622 cm^{-1}. The FT-IR spectra of MNPs/Ethyl-CN and MNPs/Ethyl-CN/Pd show Fe–O vibrations in the same vicinity. The introduction of cyano groups to the surface of MNPs is confirmed by the bands at 1009, 2245 and 2952 cm^{-1} assigned to Fe–O–Si, CN and C–H stretching vibrations, respectively. The cyanide signal appearing at 2245 cm^{-1} in Fig. 1(b) for the metal–ligand coordination[48] presumably leads to a shift of this peak to lower frequency. This shift can be observed comparing Fig. 1(c). This peak in Figs. 1(b) and (c) indicates the successful attachment of ethylcyanides organic ligands and subsequent coordination of Pd nanoparticles within the hybrid material.

The high-angle XRD patterns of Fe_3O_4 nanoparticles and Fe_3O_4/Ethyl-CN/Pd are shown in Fig. 2. It can be seen that the strong characteristic diffraction peaks at 2θ of 30.09°, 35.44°, 43.07°, 53.43°, 56.96° and 62.55° corresponding to the diffraction of (220), (311), (400), (422), (511) and (440) of Fe_3O_4 (JCPDS 89–3854) appear for both samples. This result means that the catalyst has been synthesized successfully without damaging the crystal structure of the Fe_3O_4 core. The broad peak at 2θ of 17–25° in Fig. 2(b) is assigned to the amorphous silica shell on the surface of the MNPs. Moreover, apart from the original peaks, new peaks at 2θ of 39.4°, 47.2° and 67.9°, corresponding to (111), (200) and (220) crystalline planes of Pd, are observed in the spectrum, indicating that Pd exists in the form of Pd(0), not Pd(II). The broad nature of the diffraction peak clearly indicates the Pd composition is composed of small nanocrystals, which agrees well with the TEM analysis.

TEM imaging of the Fe_3O_4/Ethyl-CN/Pd catalyst reveals that Pd nanoparticles with nearly spherical morphology are formed on the surface of the modified Fe_3O_4 nanoparticles with ethyl cyanide groups as organic shell. In the TEM images, iron oxide nanoparticles of 15–20 nm in diameter and palladium nanoparticles of *ca* 3 nm entrapped in iron oxide are observed. As shown in Fig. 3, aggregation of individual nanoparticles occurs. Such aggregations cause the difference between particle sizes derived from TEM analysis.

The presence of Pd atoms in Fe_3O_4/Ethyl-CN/Pd is also confirmed using EDS, recorded at random points on the surface for qualitative analysis (Fig. 4). The EDS spectrum also shows signals of iron, silicon and oxygen atoms, which also indicate their presence in the composite.

Figure 5 shows FESEM images of the synthesized Fe_3O_4/Ethyl-CN/Pd loaded magnetite nanoparticles. It is confirmed that the catalyst is made up of uniform nanometre-sized particles.

In combination with SEM, WDX can provide qualitative information about the distribution of various chemical elements in the catalyst matrix. Figure 6 collects representative SEM and corresponding elemental map (WDX) images for the synthesized catalyst. It can be seen that the particles are not fully spherical. In

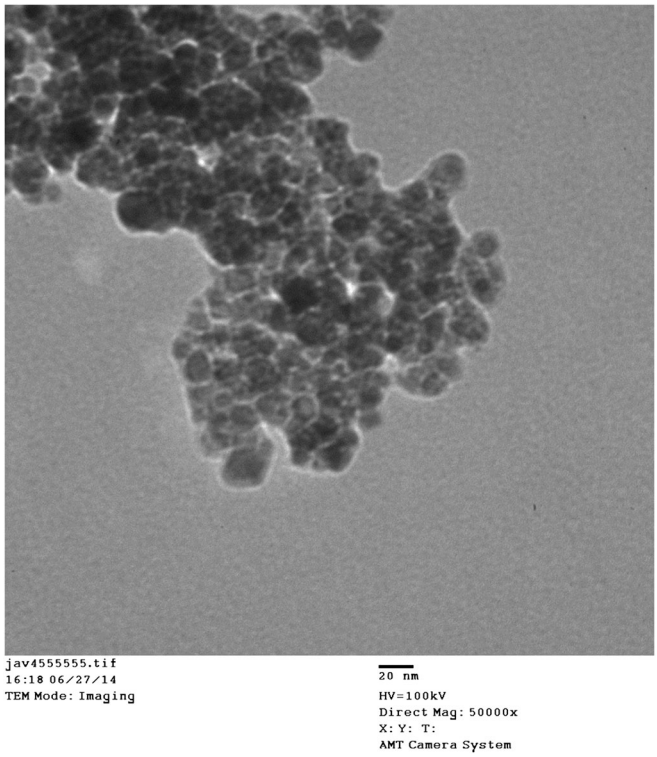

Figure 3. TEM image of Fe_3O_4/Ethyl-CN/Pd.

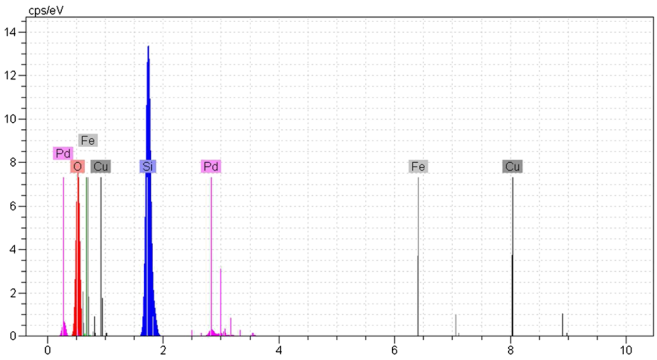

Figure 4. EDS spectrum of the catalyst.

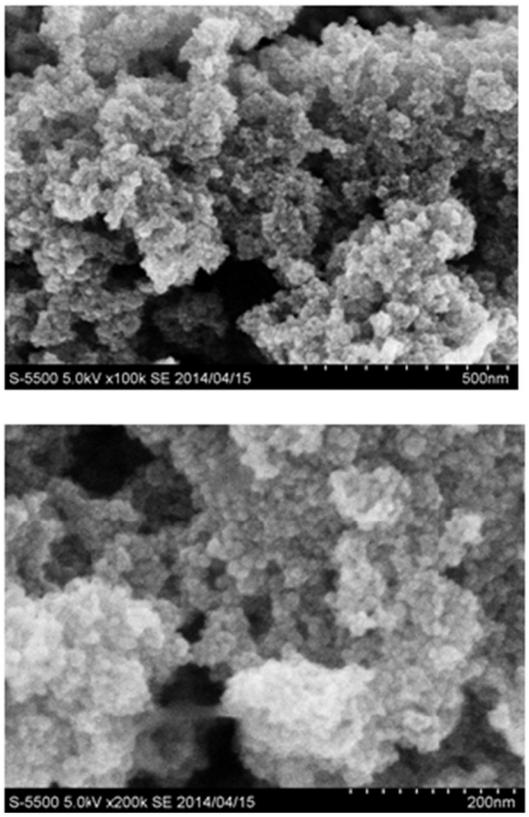

Figure 5. FESEM images of Fe_3O_4/Ethyl-CN/Pd.

addition, some particle aggregations are observed, which is likely to be caused by the magnetostatic interactions between particles. WDX analysis reveals that Pd metal particles are well dispersed in the catalyst, which agrees well with the XRD analysis.

XPS is a powerful tool for investigating the electron properties of species formed on surfaces, such as the electron environment, oxidation state and the binding energy of the core electrons of a metal. Figure 7 shows the XPS spectra of Fe_3O_4/Ethyl-CN/Pd (recorded with a Shimadzu ESCA-3400 electron spectrometer). The XPS spectrum of Fe 2p contains two peaks, strong peaks located at 712.5 and 726.8 eV, which are the typical Fe $2p_{1/2}$ and Fe $2p_{3/2}$ XPS signals of magnetite.[49] Moreover, investigation of Fe_3O_4/Ethyl-CN/Pd at the Pd 3p level shows peaks at 532.6 and 553.8 eV for Pd $3p_{3/2}$ and Pd $3p_{1/2}$, respectively, which clearly indicates that the Pd nanoparticles are stable as metallic state in the nanocomposite structure (Fig. 7). In comparison to the standard binding energy of Pd^0, with Pd $3p_{3/2}$ of about 532.4 eV and Pd $3p_{1/2}$ of about 560.2 eV,[50] it can be concluded that the Pd peaks in Fe_3O_4/Ethyl-CN/Pd shift to lower binding energy than Pd^0 standard binding energy. It has been reported that the position of the Pd 3p peak is usually influenced by the local chemical/physical environment around Pd species besides the formal oxidation state, and shifts to lower binding energy when the charge density increases.[51] Therefore, the peaks at 553.8 and 532.6 eV could be due to Pd^0 species bound directly to amino groups in Fe_3O_4/Ethyl-CN, which is in agreement with FT-IR results. The characteristic peaks corresponding to carbon (C 1s), nitrogen (N 1s) and oxygen (O 2s) are also clearly observed in XPS elemental surveys of Fe_3O_4/Ethyl-CN/Pd.

The magnetic properties of Fe_3O_4, Fe_3O_4/Ethyl-CN and Fe_3O_4/Ethyl-CN/Pd were characterized using VSM. The saturation magnetization of Fe_3O_4 nanoparticles at room temperature by measuring the magnetization curve (Fig. 8) is 62.1 emu g^{-1}; however, its minor decrease to 61.7 emu g^{-1} further suggests the formation of an ethyl cyanide coating on the surface of Fe_3O_4 nanoparticles. The M_s value

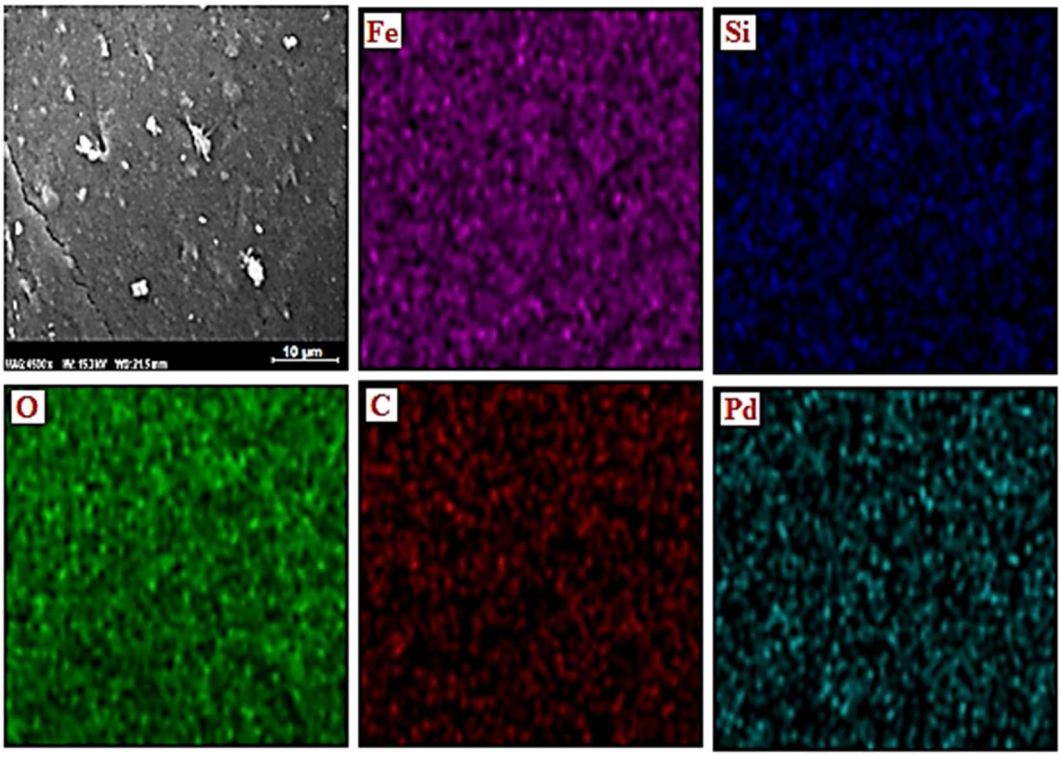

Figure 6. SEM image of Fe_3O_4/Ethyl-CN/Pd and elemental maps of Fe, Si, O, C and Pd atoms of Fe_3O_4/Ethyl-CN/Pd.

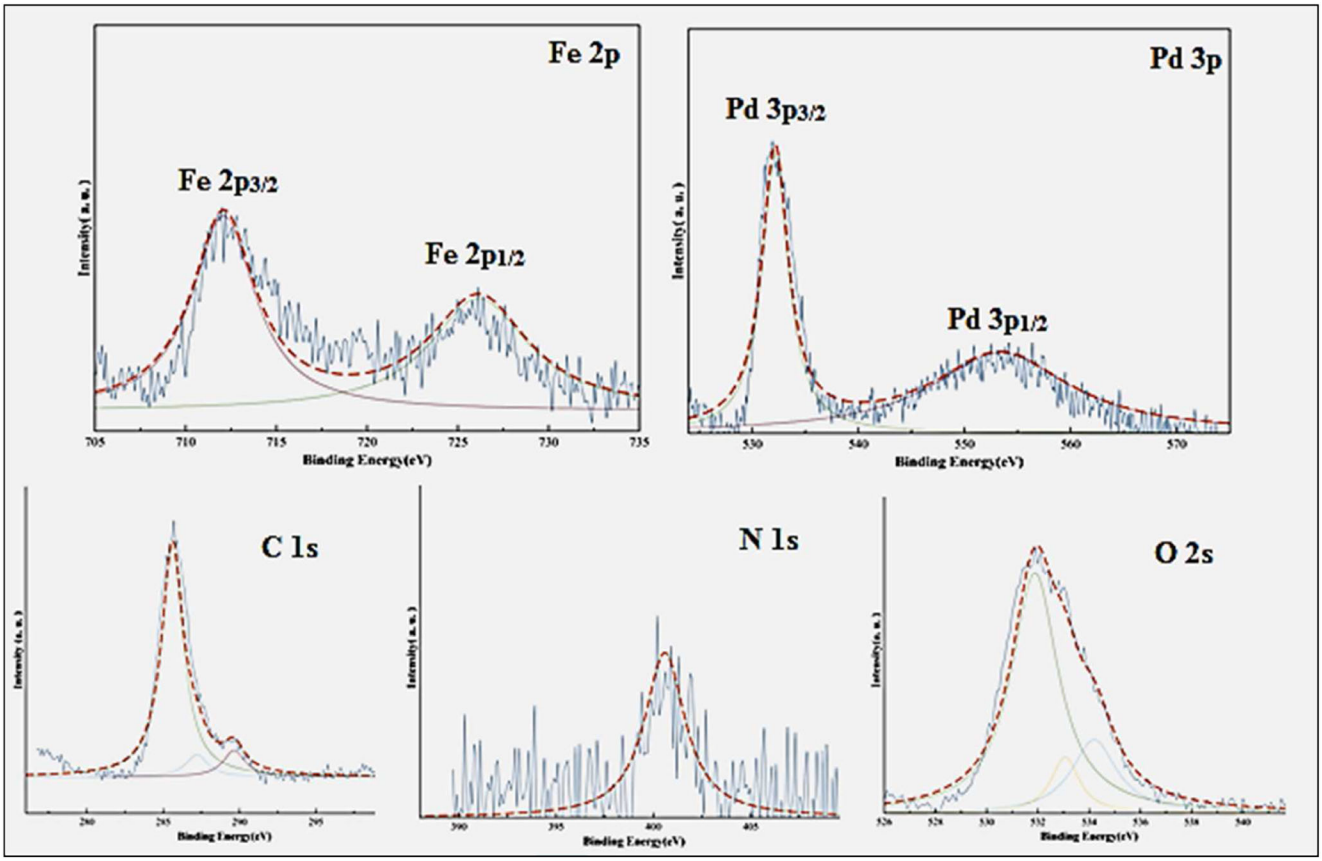

Figure 7. XPS spectra of Fe_3O_4/Ethyl-CN/Pd catalyst for Pd 3p, Fe 2p, C 1s, N 1s and O 2s.

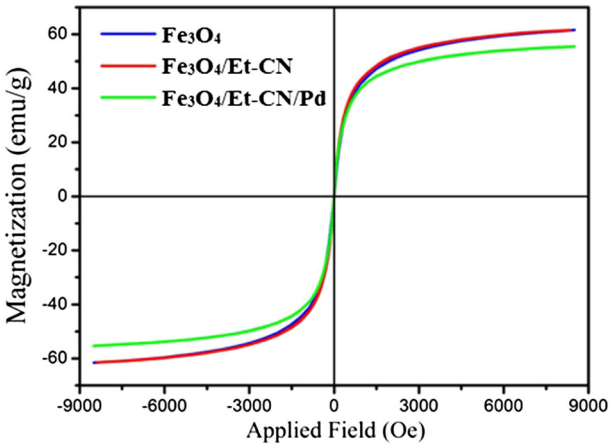

Figure 8. Room temperature magnetization curves of Fe_3O_4, Fe_3O_4/Ethyl-CN and Fe_3O_4/Ethyl-CN/Pd.

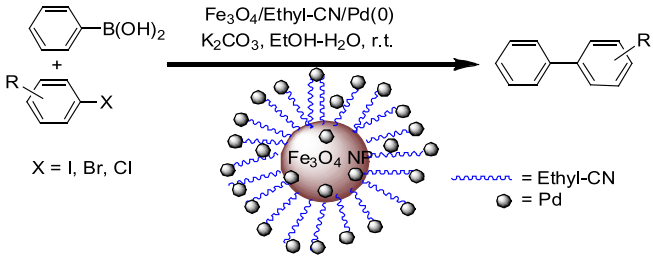

Scheme 2. Fe_3O_4/Ethyl-CN/Pd for Suzuki cross-coupling reaction.

of Fe_3O_4/Ethyl-CN/Pd is much decreased due to the Pd coating and the immobilization of Fe_3O_4/Ethyl-CN (55.3 emu g^{-1}). As a result, the modified MNPs have a typical superparamagnetic behaviour and can be efficiently attracted with a small magnet.

Fe_3O_4/Ethyl-CN/Pd was tested as a palladium magnetically separable heterogeneous nanocatalyst for the Suzuki–Miyaura coupling reaction in aqueous media under ligand-free conditions (Scheme 2). We initially selected bromobenzene and phenylboronic acid as a model reaction at room temperature. Various solvents, bases and amounts of catalyst were screened in order to establish ideal coupling conditions (Table 1). Among the bases evaluated, K_2CO_3 is found to be the most effective. H_2O–EtOH (1:1) is the best choice as solvent. The effect of catalyst loading was investigated employing various quantities of the catalyst ranging from 0.1 to 0.3 mol% (Table 1, entries 5, 8, 9). The best result is obtained with 0.007 g (0.2 mol%) of the catalyst (Table 1, entry 5).

To investigate the generality of this cross-coupling reaction, we studied the reaction of phenylboronic acid with a range of aryl halides (I, Br, Cl) under the optimized conditions (Table 2). Under the optimized conditions, phenyl iodides, bromides and chlorides all react efficiently with phenylboronic acid (Table 2, entries 1–6). Aryl halides with electron-withdrawing or electron-releasing groups react with phenylboronic acid to afford the corresponding products in high yields. It is found that the yield when using an *ortho*-substituted aryl bromide is lower (Table 2, entry 12) than when

Table 1. Optimization of conditions for the Suzuki–Miyaura reaction of bromobenzene with phenylboronic acid[a]

Entry	Solvent	Pd (mol%)	Base	Time (min)	Yield (%)[b]
1	DMF	0.2	K_2CO_3	80	82
2	Toluene	0.2	K_2CO_3	60	60
3	EtOH	0.2	K_2CO_3	60	75
4	H_2O	0.2	K_2CO_3	90	50
5	EtOH–H_2O[c]	0.2	K_2CO_3	40	98
6	EtOH–H_2O[c]	0.2	NaOAc	60	60
7	EtOH–H_2O[c]	0.2	Et_3N	90	85
8	EtOH–H_2O[c]	0.1	K_2CO_3	60	75
9	EtOH–H_2O[c]	0.3	K_2CO_3	60	96
10	EtOH–H_2O[c]	0.2	No base	90	Trace

[a]Reaction conditions: bromobenzene (1 mmol), $PhB(OH)_2$ (1.1 mmol), Fe_3O_4/Ethyl-CN/Pd, solvent (3 ml).
[b]Isolated yield.
[c]EtOH–H_2O = 1:1.

using with *para*- or *meta*-substituted aryl bromides (Table 2, entries 4–11, 13,14). Notably, heteroaryl halides such as 2-bromothiophene and 2-iodothiophene with phenylboronic acid give the corresponding coupled products in 92 and 90% yields, respectively (Table 2, entries 16 and 17).

The heterogeneity of the catalyst was evaluated to study whether the reaction using solid Pd catalyst occurs on the Fe_3O_4/Ethyl-CN surface or is catalysed by Pd species leached in the liquid phase. To address this issue, two separate experiments were conducted with bromobenzene and phenylboronic acid. In the first experiment, the reaction was terminated after 20 min; at this juncture, the catalyst was separated from the reaction mixture with an external magnet and the reaction was continued with the filtrate for an additional 40 min. In the second experiment, the reaction was terminated after 20 min. In both cases, the desired product is obtained in the same yield (40%). The result of the magnetic separation experiment confirms the heterogeneous nature of the catalyst.

So, based on these evidences and the literature,[52] a reaction mechanism for Suzuki coupling with the prepared nanocatalyst is proposed in Scheme 3. Some of the Pd(0) species bound to the support undergoes oxidative addition with the aryl halide and is released to the solution, but some still remains on the surface. After the reductive elimination step the Pd(0) is recaptured by free cyanide groups on the surface of the support and can start a new catalytic cycle. We speculate these simultaneous mechanisms are possible.

A schematic representation of the proposed catalytic route for the Suzuki reaction is presented in Scheme 3. Firstly, the aryl halide reacts with the active palladium catalyst (oxidative addition) to produce Pd(II) intermediate (**II**). Then the aryl moiety of phenylboronic acid exchanges with halide on the surface of the catalyst (**III**), and finally **III** undergoes reductive elimination to produce the expected product.

In view of industrial purposes and green chemistry, reusability of the catalyst was tested by carrying out repeated runs of the reaction on the same batch of the catalyst in the case of the model reaction (Table 1). In order to regenerate the catalyst, after each cycle, it was separated with a magnet, and washed several times with deionized water and ethanol. Then, it was dried in an oven at 50°C and used in the next run. The results show that this catalyst can be reused seven times without any significant loss in activity (Fig. 9). This high catalytic activity can be possibly related to the strong interaction of Pd nanoparticles with active sites of cyano groups. Palladium leaching of the catalyst was studied before and after the reaction using ICP-AES analysis. The Pd content is found to be 2.75 and 2.59 wt% before and after the seven reactions series, respectively, which is indicative of insignificant Pd leaching.

Table 2. Heterogeneous Suzuki–Miyaura reaction of aryl halides with phenylboronic acid catalysed by Fe_3O_4/Ethyl-CN/Pd at room temperature[a]

Entry	RC_6H_4X	X	Time (h)	Yield (%)[b]
1	H	I	0.2	98
2	H	Br	1	96
3	H	Cl	10	25
4	4-CH_3	I	0.5	98
5	4-CH_3	Br	1	90
6	4-CH_3	Cl	12	20
7	4-$COCH_3$	I	0.5	98
8	4-$COCH_3$	Br	1.5	88
9	4-CH_3O	I	0.5	95
10	4-CH_3O	Br	2	90
11	4-Cl	Br	0.8	98
12	2-CHO	Br	4	88
13	3-NO_2	I	1	92
14	3-NO_2	Br	5	80
15	1-Naphthyl	I	1	96
16	2-Thienyl	I	2	90
17	2-Thienyl	Br	6	92

[a]Reactions were carried out under aerobic conditions in 3 ml of H_2O–EtOH (1:1), 1.0 mmol arylhalide,1.1 mmol phenylboronic acid and 2 mmol K_2CO_3 in the presence of catalyst (0.007 g, 0.2 mol% Pd).
[b]Isolated yield.

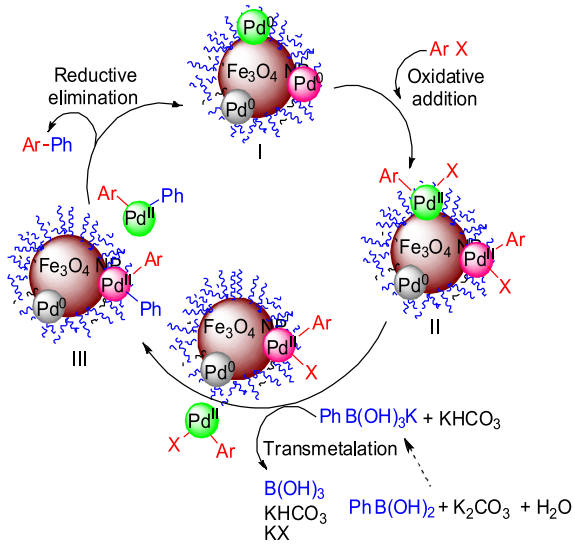

Scheme 3. Possible mechanism of Suzuki coupling reaction using Fe_3O_4/Ethyl-CN/Pd.

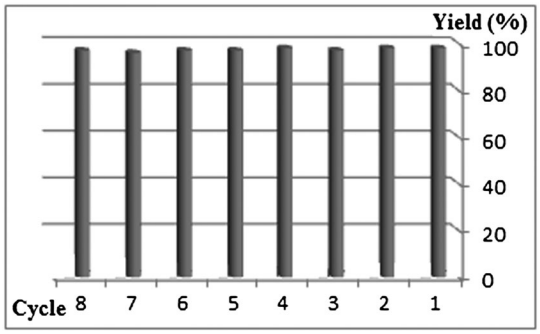

Figure 9. Recycling of Fe_3O_4/Ethyl-CN/Pd for the Suzuki coupling reaction under similar conditions.

Conclusions

We have developed an efficient protocol for the preparation of Fe_3O_4/Ethyl-CN/Pd nanoparticles. The catalyst was characterized using FT-IR, XRD, FESEM, TEM, VSM, WDX, ICP, EDS and XPS analyses. The heterogeneous catalyst demonstrates good catalytically performance in the Suzuki coupling reaction. The advantageous features of the proposed methodology include generality, high efficiency and simplicity, which lead to short reaction times, high yields, cleaner reaction profile and easy reusability of the heterogeneous catalyst using a magnet. These unique results open new perspectives for the application of these types of magnetic catalysts in other organic reactions.

Acknowledgements

We are grateful to Islamic Azad University of Tonekabon and Payame Noor University for partial support of this work.

References

[1] N. Miyaura, A. Suzuki, *Chem. Rev.* **1995**, *95*, 2457.
[2] A. Suzuki, *J. Organometal. Chem.* **1999**, *576*, 147.
[3] A. F. Littke, G. C. Fu, *Angew. Chem. Int. Ed.* **2002**, *41*, 4176.
[4] a) L. Yin, J. Liebscher, *Chem. Rev.* **2007**, *107*, 133 and references therein; b) H. Li, L. Wang, P. Li, *Synthesis* **2007**, *39*, 1635; c) V. Budarin, J. H. Clark, J. J. E. Hardy, R. Luque, K. Milkowski, S. J. Tavener, A. J. Wilson, *Angew. Chem. Int. Ed.* **2006**, *45*, 3782; dd) D. Choudhary, S. Paul, R. Gupta, J. H. Clark, *Green Chem.* **2006**, 8, 479 and references therein.
[5] a) W. Chen, Z. Huang, Y. Liu, Q. He, *Catal. Commun.* **2008**, *9*, 516; b) A. Solhy, J. H. Clark, R. Tahir, S. Sebti, M. Larzek, *Green Chem.* **2006**, *8*, 871; c) D. Mahajan, B. A. Ganai, R. L. Sharma, K. K. Kapoor, *Tetrahedron Lett.* **2006**, *47*, 7919.
[6] a) K. Mori, K. Yamaguchi, T. Hara, T. Mizugaki, K. Ebitani, K. Kaneda, *J. Am. Chem. Soc.* **2002**, *124*, 11572; b) T. Hara, K. Mori, M. Oshiba, T. Mizugaki, K. Ebitani, K. Kaneda, *Green Chem.* **2004**, *6*, 507; c) K. Mori, T. Hara, M. Oshiba, T. Mizugaki, K. Ebitani, K. Kaneda, *New J. Chem.* **2005**, *29*, 1174.
[7] a) A. Suzuki, N. Miyaura, *Chem. Rev.* **1995**, *95*, 2457; b) A. Suzuki, *J. Organometal. Chem.* **2002**, *653*, 83; c) S. P. Stanforth, *Tetrahedron* **1998**, *54*, 263.
[8] a) D. A. Horton, G. T. Bourne, M. L. Smythe, *Chem. Rev.* **2003**, *103*, 893; b) P. J. Hajduk, M. Bures, J. Praestgaard, S. W. Fesik, *J. Med. Chem.* **2000**, *43*, 3443; c) K. F. Croom, G. M. Keating, *Am. J. Cardiovasc. Drugs* **2004**, *4*, 395.
[9] a) C. Fleckenstein, S. Roy, S. Leuthauber, H. Plenio, *Chem. Commun.* **2007**, *42*, 2870; b) F. Churruca, R. SanMartin, B. Inés, I. Tellitu, E. Domínguez, *Adv. Synth. Catal.* **2006**, *348*, 1836; c) Q. Yang, S. Ma, J. Li, F. Xiao, H. Xiang, *Chem. Commun.* **2006**, *41*, 2495.
[10] H. Wu, C. Wu, Q. He, X. Liao, B. Shi, *Mater. Sci. Eng. C* **2010**, *30*, 770.
[11] J. H. Xia, H. Shen, B. F. Shu, W. Zhang, *Mater. Res. Bull.* **2008**, *43*, 2213.
[12] T. Matsunaga, H. Takeyama, *Science* **1998**, *5*, 391.
[13] S. Sun, C. Murray, D. Weller, L. Folks, A. Moser, *Science* **2000**, *287*, 1989.
[14] E. H. Kim, Y. Ahn, H. S. Lee, *J. Alloys Compd.* **2007**, *434–435*, 633.
[15] M. Racuciu, D. E. Creanga, G. Calugaru, *J. Optoelectron. Adv. Mater.* **2005**, *7*, 2859.
[16] S. Tang, L. Wang, Y. Zhang, S. Li, S. Tian, B. Wang, *Fuel Process. Technol.* **2012**, *95*, 84.
[17] B. V. Subba Reddy, A. Siva Krishna, A. V. Ganesh, G. G. K. S. Narayana Kumar, *Tetrahedron Lett.* **2011**, *52*, 1359.
[18] R. Parella, N. Srinivasarao, A. Babu, *Catal. Commun.* **2012**, *29*, 118.
[19] H. Niu, Z. Meng Dizhang, Y. Cai, *J. Hazard. Mater.* **2012**, *227–228*, 195.
[20] H. Liu, Z. Jia, S. Ji, Y. Zheng, M. Li, H. Yang, *Catal. Today* **2011**, *175*, 293.
[21] L. Ai, C. Zeng, Q. Wang, *Catal. Commun.* **2011**, *14*, 68.
[22] A. Kong, P. Wang, H. Zhang, F. Yang, S. Huang, Y. Shan, *Appl. Catal. A* **2012**, *417*, 183.
[23] J. Liu, Y. Zhou, F. Liu, C. Liu, J. Wang, Y. Pan, D. Xue, *RSC Adv.* **2012**, *2*, 2262.
[24] G. Li, L. Mao, *RSC Adv.* **2012**, *2*, 5108.
[25] Y. Ke, Y. Zeng, X. Pu, X. Wu, L. Li, Z. Zhu, Y. Yu, *RSC Adv.* **2012**, *1*, 5676.
[26] Z. Wang, B. Shen, Z. Aihua, N. He, *Chem. Eng. J.* **2005**, *113*, 27.
[27] F. Zhang, J. Niu, H. Wang, H. Yang, J. Jin, N. Liu, Y. Zhang, R. Li, J. Ma, *Mater. Res. Bull.* **2012**, *47*, 504.
[28] M. Ma, Q. Zhang, D. Yin, J. Dou, H. Zhang, H. Xu, *Catal. Commun.* **2012**, *17*, 168.
[29] Q. Du, W. Zhang, H. Ma, J. Zheng, B. Zhou, Y. Li, *Tetrahedron* **2012**, *68*, 3577.
[30] Z. Wang, P. Xiao, B. Shen, N. He, *Colloid Surf. A* **2006**, *276*, 116.
[31] Z. Yinghuai, S. C. Peng, A. Emi, S. Zhenshun, R. A. Kemp, *Adv. Synth. Catal.* **2007**, *349*, 1917.
[32] P. Li, L. Wang, L. Zhang, G. W. Wang, *Adv. Synth. Catal.* **2012**, *354*, 1307.
[33] A. N. Ay, N. V. Abramova, D. Konuk, O. L. Lependina, V. I. Sokolov, B. Z. Karan, *Inorg. Chem. Commun.* **2013**, *27*, 64.
[34] a) D. Astruc, F. Lu, J. R. Aranzaes, *Angew. Chem. Int. Ed. Engl.* **2005**, *44*, 7852; b) C. Deraedt, D. Wang, L. Salmon, L. Etienne, C. Labrugère, J. Ruiz, D. Astruc, *ChemCatChem* **2015**, *7*, 303; c) D. Wang, D. Astruc, *Chem. Rev.* **2014**, *114*, 6949.
[35] B. Sreedhar, S. Kumar, D. Yada, *Synthesis* **2011**, *8*, 1081.
[36] S. Li, W. Zhang, M.-H. So, C.-M. Chi-Ming Che, R. Wang, R. Chen, *J. Mol. Catal. A* **2012**, *359*, 81.
[37] F. Zamani, S. M. Hossein, *Catal. Commun.* **2014**, *43*, 164.
[38] H. Veisi, P. Mohammadi, J. Gholami, *Appl. Organometal. Chem.* **2014**, *28*, 868.
[39] R. Ghorbani-Vaghei, M. Chegini, H. Veisi, M. Karimi-Tabar, *Tetrahedron Lett.* **2009**, *50*, 1861.
[40] H. Veisi, M. Hamelian, S. Hemmati, *J. Mol. Catal. A* **2014**, *395*, 25.
[41] R. Ghorbani-Vaghei, H. Veisi, *Synthesis* **2009**, *6*, 945.
[42] H. Veisi, J. Gholami, H. Ueda, P. Mohammadi, M. Noroozi, *J. Mol. Catal. A* **2015**, *396*, 216.
[43] B. Maleki, D. Azarifar, H. Veisi, S. F. Hojati, H. Salehabadi, R. Nejat Yami, *Chin. Chem. Lett.* **2010**, *21*, 1346.
[44] S. Luo, X. Zheng, H. Xu, X. Mi, L. Zhang, J.-P. Cheng, *Adv. Synth. Catal.* **2007**, *349*, 2431.
[45] M. Z. Kassaee, H. Masrouri, F. Movahed, *Appl. Catal. A* **2011**, *395*, 28.
[46] Z. M. Rao, T. H. Wu, S. Y. Peng, *Acta Phys. Chim. Sin.* **1995**, *11*, 395.
[47] R. D. Waldron, *Phys. Rev.* **1955**, *99*, 1727.
[48] A. D. Becke, *J. Chem. Phys.* **1996**, *104*, 1040.
[49] D. Zhang, Z. Liu, S. Han, C. Li, B. Lei, M. P. Stewart, J. M. Tour, C. Zhou, *Nano Lett.* **2004**, *4*, 2151.
[50] M. C. Militello, S. J. Simko, *Surf. Sci. Spectra* **1994**, *3*, 387.
[51] T. Teranishi, M. Miyake, *Chem. Mater.* **1998**, *10*, 594.
[52] a) A. F. Schmidt, A. A. Kurokhtina, *Kinetics Catal.* **2012**, *53*, 714; b) D. Wang, C. Deraedt, L. Salmon, C. Labrugère, L. Etienne, J. Ruiz, D. Astruc, *Chem. Eur. J.* **2015**, *21*, 1508; c) A. K. Diallo, C. Ornelas, L. Salmon, J. Ruiz Aranzaes, D. Astruc, *Angew. Chem. Int. Ed. Engl.* **2007**, *46*, 8644.

